

Supporting Information

Ultrathin Cuprite Film on Pt(111) with High Reactivity to CO

Wenyuan Wang,^{†,§} Zhilin Wen,^{‡,§} Shanwei Hu,[¶] Zhe Li,[†] Xiaojun Wu,^{‡,*} Junfa Zhu[¶] and Xiang Shao^{†,*}

[†] Department of Chemical Physics, University of Science and Technology of China, Hefei, Anhui 230026, P. R. China

[‡] Hefei National Laboratory of Physical Sciences at the Microscale, CAS Key Laboratory of Materials for Energy Conversion, CAS Excellence in Nanoscience, and School of Chemistry and Materials Sciences, University of Science and Technology of China, Hefei, Anhui 230026, P. R. China

[¶] National Synchrotron Radiation Laboratory, University of Science and Technology of China, Hefei, Anhui 230026, P. R. China

[§] These authors contributed equally to this work.

To whom correspondence should be addressed: shaox@ustc.edu.cn; xjwu@ustc.edu.cn

1. Experimental methods

STM studies were conducted on a commercial low-temperature STM system (Createc Co.) equipped with LEED, AES, surface cleaning facilities, and metal evaporators. The base pressure of the preparation chamber is about 1×10^{-10} mbar while that of the STM chamber better than 6×10^{-11} mbar. The atomically flat Pt(111) surface was achieved by repeated cycles of Ar⁺ sputtering at RT and vacuum-annealing at temperatures around 1200 K. When needed, the sample was annealed in 5×10^{-8} mbar O₂ at ~850 K to remove any carbon species on the surface. The copper oxide film was prepared by depositing elemental Cu from an home-made evaporator onto the as-prepared Pt(111) surface which was held at RT followed by annealing to ~550 K in 1×10^{-6} mbar O₂. The applied gases, O₂ and CO (Air Product, 99.999%), were all introduced by background feeding through variable leak valves. All STM measurements were conducted at liquid nitrogen temperature (77 K) with an electrochemically etched tungsten tip. All images were collected in constant current mode.

The XPS and TPD measurements were performed at the “Catalysis and Surface Science End-station” at the BL11U beamline in the National Synchrotron Radiation Laboratory (NSRL). The beamline is connected to an undulator and equipped with two gratings that offer soft X-rays from 20 to 600 eV with a resolution (E/ΔE) better than 10⁴ at 29 eV. Detailed descriptions of these two systems could be found in our previous works.¹⁻² The preparation of the Cu₂O/Pt(111) sample and its reaction with CO were carried out at separated chamber equipped with an e-beam Cu evaporator and CO doser. The experimental procedures were completely copied from that applied on our STM system. After CO exposure, the sample was frozen to ~100 K before transferring to the analysis chamber for XPS measurements. Noticeably, the C 1s spectra were acquired with synchrotron radiation photons with energy of 400 eV whereas the O 1s, Cu 2p and Auger spectroscopy were collected with an ESCALab 250 X-ray photoelectron spectrometer, using monochromatized Al-Kα X-ray as the excitation source. The XPS data were analyzed with the XPSPEAK program. The O1s and C1s peak positions were fitted with mixed Lorentzian–Gaussian curves after removing a linear background. The Pt 4f electronic states were applied as internal reference.

TPD experiments were conducted in an ultrahigh vacuum chamber with base pressure below 5×10^{-10} Torr. CO gas (Air Product, 99.999%) was introduced by background feeding through a variable leak valve. During exposure, the sample was held at 130 K. The sample was heated with a steady rate of 1 K/s until 550 K. The desorbed molecules were detected by a differentially pumped mass spectrometer (Hidden Co.)

equipped with a collection cone which approaches as ~3 mm as close to the sample surface.

2. Computational methods

All calculations were carried out using the Vienna ab Initio Simulation Package (VASP)³⁻⁴ based on the density function theory (DFT) with projector augmented wave potentials.⁵⁻⁶ Exchange and correlation energies were treated in the generalized gradient approximation (GGA) of Perdew Burke Ernzerhof (PBE).⁷ All calculations were done with a 500 eV kinetic energy cutoff for a plane wave basis set, and the atomic structures were fully optimized until the forces were smaller than $|0.05| \text{ eV/\AA}$ and the energy changes were smaller than 10^{-5} eV. To model the structure of Cu_2O films on Pt, a (3×3) $\text{Cu}_2\text{O}(111)$ -like layer overlapping on a two-layered (10×10) slab of Pt(111) with $(\sqrt{43} \times \sqrt{43}) - R7.6^\circ$ registry was constructed. The k-points were sampled with $(2 \times 2 \times 1)$ grids, which is reasonable considering the large size of our slab ($a = b = 18.442 \text{ \AA}$) and the ignorable difference (about 1 meV/atom) against the convergence test with larger grids of $(3 \times 3 \times 1)$ and $(4 \times 4 \times 1)$. It is worth mentioning that the structure of $\text{Cu}_2\text{O}(111)$ -like layer was obtained by removal of Cu atoms in the center of hexagonal rings of an intrinsic $\text{Cu}_2\text{O}(111)$ surface. The bottom layer of the Pt substrate was fixed and the other layers were allowed to relax during the structural optimization. A vacuum layer of more than 15 \AA for all models was used to avoid the interactions between periodically repeated slabs. The computational STM images were generated by using the constant current model, which is implemented in the p4vasp program using the Tersoff–Hamann approach.⁸⁻⁹

For the simulation of oxidation reaction of CO at the periphery of Cu_2O island on Pt(111), we used a $(1 \times 2 \times 1)$ $\text{Cu}_2\text{O}/\text{Pt}$ slab and removed half of the $\text{Cu}_2\text{O}(111)$ -like layer to model the boundary. The adsorption energy of CO molecule is defined as:

$$E_{\text{ads}}(\text{CO}) = E_{\text{CO/surf}} - E_{\text{CO}} - E_{\text{surf}}$$

in which E_{CO} , E_{surf} , and $E_{\text{CO/surf}}$ are the total energies of CO in the gas phase, the clean surface of $\text{Cu}_2\text{O}/\text{Pt}(111)$, and the optimized adsorbate/surface system, respectively. The reaction energy (E_r) of the elementary step was calculated by using the total energy difference between products/substrate and reactants/substrate. Here negative values of E_{ads} and E_r indicate an exothermic and energetically favorable process. The climbing image nudged elastic band (CI-NEB)¹⁰ and dimer method¹¹ were used to calculate the activation energy barriers for the CO oxidation, with the transition states (TSs) verified through a rigorous vibrational frequency analysis. The activation energy (E_a) is determined by the energy difference between the transition state and initial state in each corresponding reaction step. In addition, all total energies were extrapolated to zero temperature without including a zero-point energy correction.

3. Additional figures:

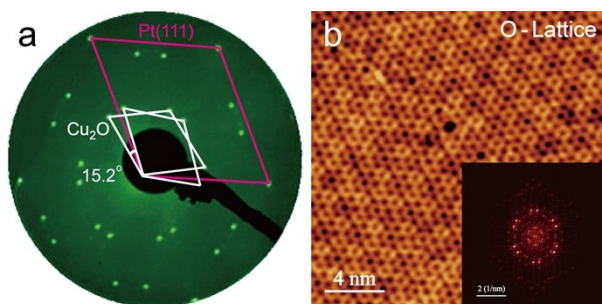


Fig. S1. (a) LEED pattern of the as-prepared Cu_2O film on Pt(111). Pink and bright rhombics define the Pt(111) and the $\text{Cu}_2\text{O}(111)$ lattice, respectively. (b) Oxygen-resolved high-resolution STM image of the $\text{Cu}_2\text{O}/\text{Pt}(111)$ film with a boundary region separating two differently rotated domains. Inset shows the FFT pattern of the image, clearly presenting two set of lattice with hexagonal symmetry. The distortion of the lattice is due to the thermal drift. Tunneling condition: $U_s = -1.2$ V, $I = 1.2$ nA.

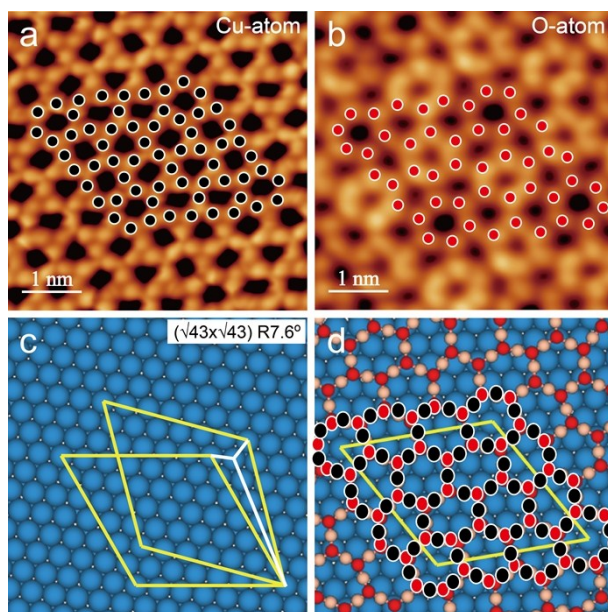


Fig. S2. (a) Cu-resolved and (b) O-resolved high-resolution STM images of exactly the same area (10×10 nm²) overlapped with black and red circles showing the atom positions, respectively. Tunneling conditions are (a) $U_s = 0.008$ V, and (b) $I = 8.0$ nA $U_s = -1.2$ V, $I = 0.98$ nA. (c) is the structural model for the Pt(111) substrate. Yellow rhombics indicate the unit cell of the overlayers with different rotational registry. (d) is the model of the $\text{Cu}_2\text{O}/\text{Pt}(111)$ film with one rotational registry and overlaid with the black and red circles from (a) and (b), showing perfectly consistency. The blue, orange and red balls represent Pt, Cu and O atoms, respectively.

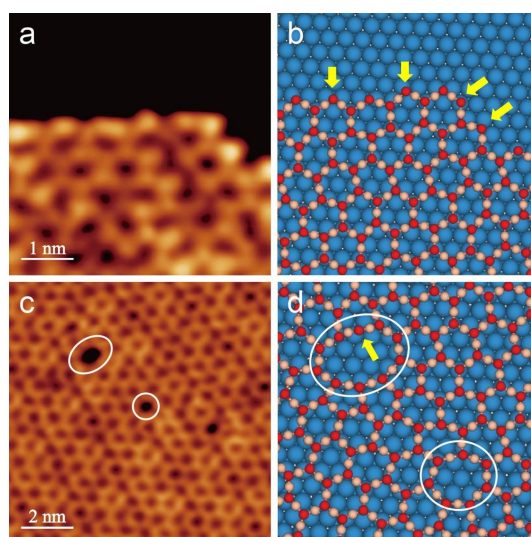


Fig. S3. (a,c) High resolution STM image and (b,d) the STM-derived models of the periphery (a,b) and the defects (c,d) of the Cu_2O island on the $\text{Pt}(111)$ surface. One can clearly see the two-fold coordinated oxygen sites (O_{cus} , yellow arrows) in these positions. Tunneling condition: $U_s = 0.35$ V, $I = 0.16$ nA.

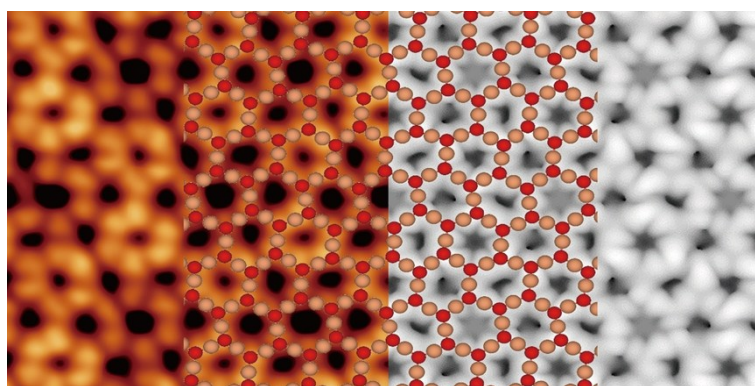


Fig. S4. Oxygen-resolved high resolution STM image of the $\text{Cu}_2\text{O}/\text{Pt}(111)$ film overlapped with the model (middle) and the simulated STM image, showing very good consistency.

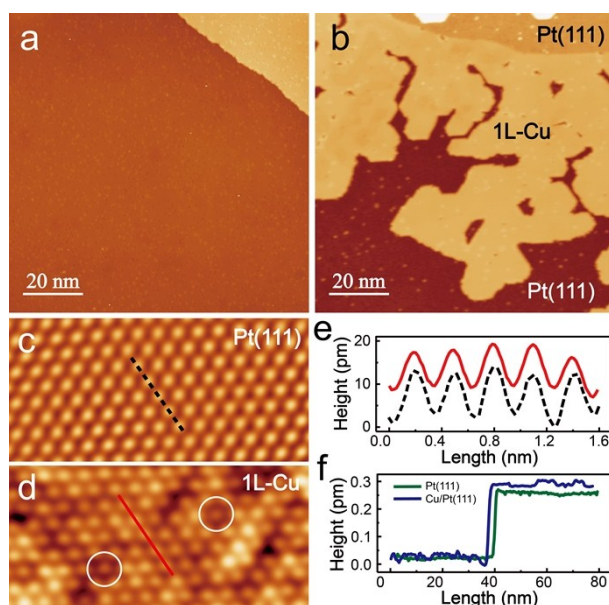


Fig. S5. STM images of (a) clean Pt(111) and (b) with 0.3 ML Cu film evaporated at room temperature. (c) and (d) are atomic resolution images of Pt(111) substrate and the Cu film ($2.4 \times 5 \text{ nm}^2$), showing the same lattice orientation. (e) shows the profiles along the black and red lines in (c) and (d), respectively, showing exactly the same lattice constant. (f) Height profiles across a Pt step (green) and the boundary of Cu island (blue). Tunneling conditions are (a) $U_s = 0.26 \text{ V}$, $I = 0.78 \text{ nA}$, (b) $U_s = 1.18 \text{ V}$, $I = 0.1 \text{ nA}$, (c) $U_s = -0.008 \text{ V}$, $I = 3.3 \text{ nA}$, and (d) $U_s = -0.008 \text{ V}$, $I = 3.2 \text{ nA}$.

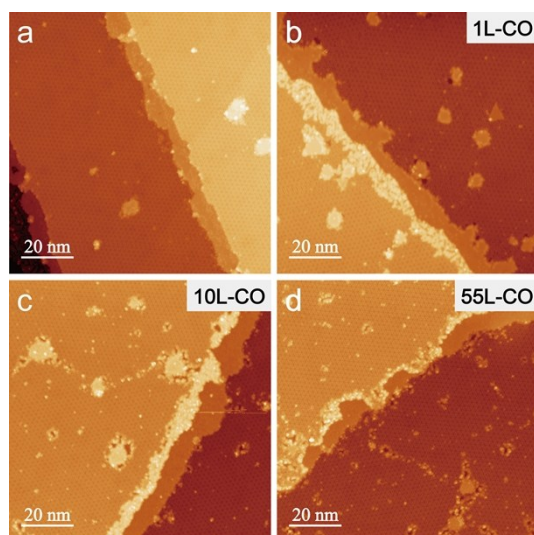


Fig. S6. STM image of (a) the as-prepared Cu₂O/Pt(111) film and after exposing to (b) 1L, (c) 10 L and (d) 55 L of CO at 200 K. The corrosion at the defect/boundary sites is obvious, but the propagation of the reaction is rather slow at such low temperature. Tunneling conditions are (a) $U_s = 1.03 \text{ V}$, $I = 0.15 \text{ nA}$, (b) $U_s = -0.42 \text{ V}$, $I = 1.3 \text{ nA}$, (c) $U_s = -0.43 \text{ V}$, $I = 0.16 \text{ nA}$, and (d) $U_s = -0.87 \text{ V}$, $I = 0.17 \text{ nA}$.

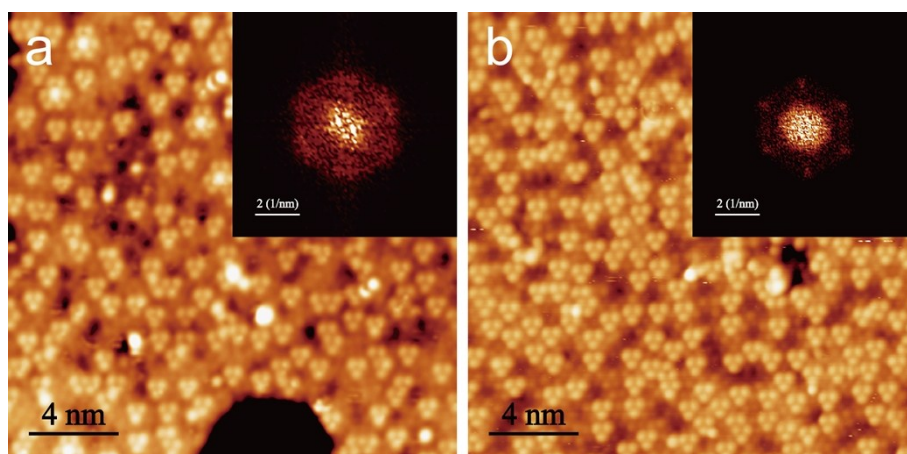


Fig. S7. STM images of (a) the reduced $\text{Cu}_2\text{O}(111)/\text{Pt}$ film and (b) the $\text{Cu}/\text{Pt}(111)$ film after exposure of 3.5 L O_2 at room temperature. This result strongly supports the proposition that the $\text{Cu}_2\text{O}/\text{Pt}$ film is reduced by CO to form Cu adlayer with chemisorbed oxygen which forms a (2×2) superstructure. Insets are the corresponding FFT patterns showing the same hexagonal symmetry, also supporting the consistency of the oxygen adsorption structure on the produced Cu island. Tunneling conditions: (a) $U_s = -0.55$ V, $I = 0.5$ nA; (b) $U_s = -0.19$ V, $I = 2.6$ nA.

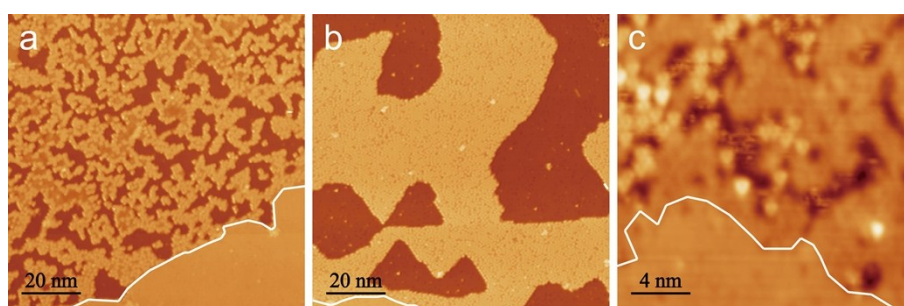


Fig. S8. STM images of the $\text{Cu}_2\text{O}/\text{Pt}(111)$ film (a) after exposing 15 L of CO at RT, (b) followed by subsequent heating to 500 K for 2 min and (c) for another 3 min. Notice upon annealing, the produced Cu islands aggregate into large patches. The chemisorbed oxygen also desorbs at this temperature. But the 3LP features are more thermally stable hence can survive partially even after 5 min annealing. The white curves mark the boundaries of the Cu_2O -red film and $\text{Pt}(111)$ steps. Tunneling conditions: (a) $U_s = -0.88$ V, $I = 0.97$ nA, (b) $U_s = -0.49$ V, $I = 1.5$ nA, (c) $U_s = -0.33$ V, $I = 1.3$ nA.

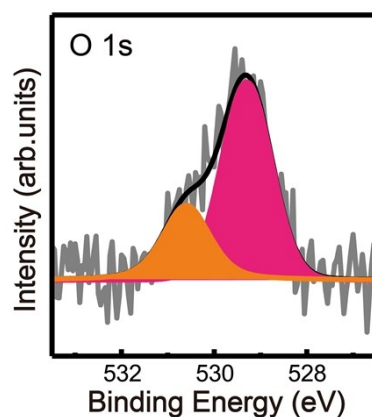


Fig. S9. O 1s XPS spectrum obtained on the Cu/Pt(111) film after O₂ exposure at room temperature, corresponding to the STM image in Fig. S7b shown above. The deconvoluted rose red peak (□529.3 eV) corresponds to the chemisorbed oxygen organized in a (2×2) superstructure while the orange peak (□530.6 eV) corresponds to the subsurface oxygen involved in the 3LP species.

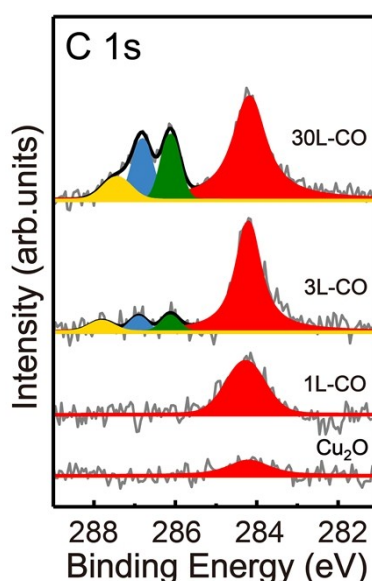


Fig. S10. C 1s PES spectra for the Cu₂O/Pt(111) film after exposing to different amounts of CO. These spectra were collected at the synchrotron end-station with the photo energy of 400 eV. The blue and green peaks are attributed to CO adsorption on top sites and bridge sites of the Pt(111) surface, respectively, indicating the gradually exposed Pt(111) surface upon reduction of the Cu₂O film. The yellow peak is tentatively attributed to CO adsorbed at the boundary of Cu₂O/Pt(111). The red peak, which appeared at the beginning and grew with the experimental procedure, is assigned to the accumulated carbon species on the sample surface.

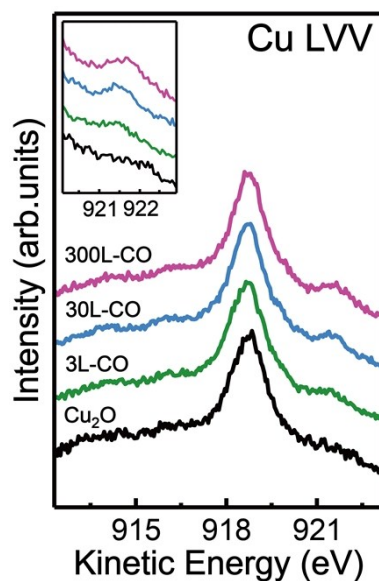


Fig. S11. Cu_{LVV} Auger spectra of the $\text{Cu}_2\text{O}/\text{Pt}(111)$ film after exposing to different amounts of CO at 300 K. Inset shows the change of the AES satellite features around 921.5 eV which demonstrates the gradual reduction of the Cu_2O film.

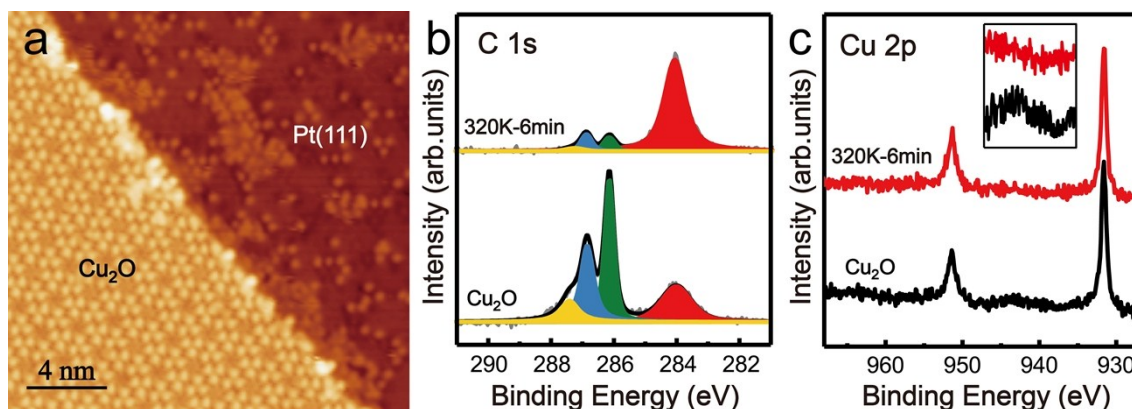


Fig. S12. (a) STM image of $\text{Cu}_2\text{O}/\text{Pt}(111)$ film after CO exposure at 77 K. The bright dots on the exposed $\text{Pt}(111)$ region are the chemisorbed CO molecules. In contrast, on the Cu_2O film no CO can be observed. Tunneling condition: $U_s = -0.5$ V, $I = 2.1$ nA. (b) and (c) show the C 1s, and Cu 2p XPS spectra for the $\text{Cu}_2\text{O}/\text{Pt}(111)$ film with CO pre-dosed at 100 K (black curve) and followed by subsequent heating to 320 K for 6 minutes in vacuum (red curve), respectively. Concerning the deconvolution of C1s in (b), the assignments are the same as those in Fig. S10 shown above.

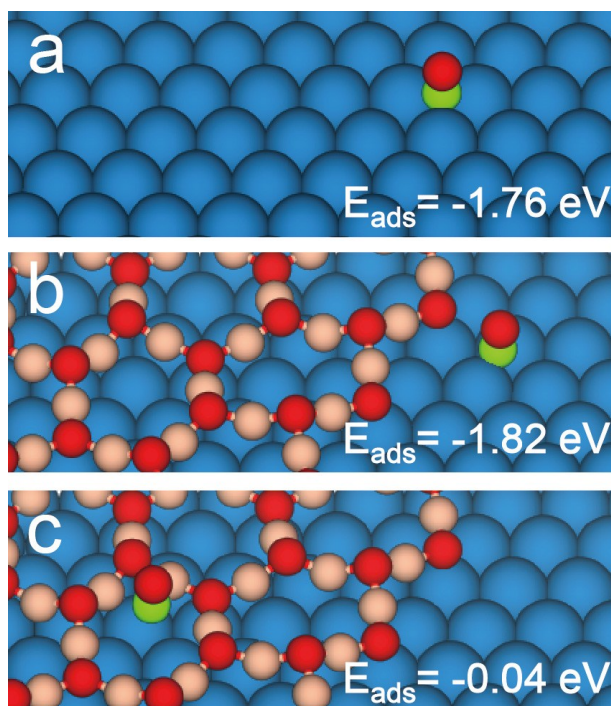


Fig. S13. Calculated adsorption configurations and corresponding adsorption energies of CO on (a) Pt(111) substrate, (b) the periphery of Cu₂O/Pt(111) island and (c) inside hexagonal pore of the Cu₂O/Pt(111) film. Notice the wrong prediction of CO adsorption site on Pt(111) is well known. But the calculated adsorption energy is reliable. Pt, Cu, C and O atoms are shown in dark blue, powder orange, gray and red, respectively. The carbon atom of CO is blocked by the oxygen atom due to top-down view point.

Notes and references

- 1 W. Wang, S. Hu, Y. Han, X. Pan, Q. Xu, J. Zhu, *Surf. Sci.*, 2016, **653**, 205.
- 2 Q. Xu, S. Hu, D. Cheng, X. Feng, Y. Han, J. Zhu, *J. Chem. Phys.*, 2012, **136**, 154705.
- 3 G. Kresse, J. Furthmüller, *Phys. Rev. B*, 1996, **54**, 11169.
- 4 G. Kresse, J. Furthmüller, *Comp. Mater. Sci.*, 1996, **6**, 15.
- 5 P. E. Blöchl, *Phys. Rev. B*, 1994, **50**, 17953.
- 6 G. Kresse, D. Joubert, *Phys. Rev. B*, 1999, **59**, 1758.
- 7 J. P. Perdew, K. Burke, M. Ernzerhof, *Phys. Rev. Lett.*, 1996, **77**, 3865.
- 8 J. Tersoff, D. R. Hamann, *Phys. Rev. B*, 1985, **31**, 805.
- 9 J. Tersoff, D. R. Hamann, *Phys. Rev. Lett.*, 1983, **50**, 1998.
- 10 G. Henkelman, B. P. Uberuaga, H. Jónsson, *J. Chem. Phys.*, 2000, **113**, 9901.
- 11 G. Henkelman, H. Jónsson, *J. Chem. Phys.*, 1999, **111**, 7010.